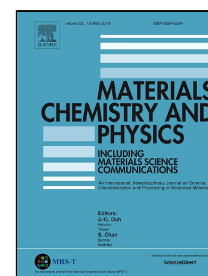# Accepted Manuscript

A facilitated synthesis of hierarchically porous Cu-Ce-Zr catalyst using bacterial cellulose for VOCs oxidation

Baojuan Dou, Ruozhu Zhao, Ningna Yan, Chenchen Zhao, Qinglan Hao, Oscar KS. Hui, Kwun Nam Hui

Please cite this article as: Baojuan Dou, Ruozhu Zhao, Ningna Yan, Chenchen Zhao, Qinglan Hao, Oscar KS. Hui, Kwun Nam Hui, A facilitated synthesis of hierarchically porous Cu-Ce-Zr catalyst using bacterial cellulose for VOCs oxidation, *Materials Chemistry and Physics* (2019), doi: 10.1016/j.matchemphys.2019.121852

A facilitated synthesis of hierarchically porous Cu-Ce-Zr catalyst using bacterial cellulose for VOCs oxidation

Baojuan Dou [a], Ruozhu Zhao [a], Ningna Yan [a], Chenchen Zhao [a], Qinglan Hao [a*],

Oscar KS Hui [b*], Kwun Nam Hui [c]

[a] Tianjin University of Science & Technology, Tianjin 300457, China;

[b] Mechanical Engineering Engineering, Faculty of Science, University of East Anglia,

Norwich Research Park, NR4 7TJ, UK

[c] Institute of Applied Physics and Materials Engineering, University of Macau,

Avenida da Universidade, Taipa, Macau, China

 Corresponding author

Qinglan Hao, E-mail: haoqinglan@tust.edu.cn, Tel: +86 22 60600300

Oscar KS Hui, E-mail: k.hui@uea.ac.uk, Fax: +44 01603 59 2582

Abstract: Highly active $CuO-CeO_2-ZrO_2$ catalysts were prepared by sol-gel method, using environmentally friendly bacterial cellulose (BC) as structure directing regent.

The catalyst designed with commercial BC (Com-BC) exhibited catalytic performances in toluene (T_{100} =220 °C) and ethyl acetate oxidation (T_{100} =170 °C) superior to the catalysts prepared by traditional methods. Furthermore, excellent stability was obtained and no deactivation was observed during the 100 h on stream in toluene and ethyl acetate oxidation at T_{100}. The excellent activity and stability of Com-BC can be explained by the hierarchically porous structure, abundant oxygen vacancies, and good reducibility.

Keywords: Volatile organic compounds; Cu-Ce-Zr catalyst; bacterial cellulose; hierarchical pore; catalytic oxidation

1. Introduction

Volatile organic compounds (VOCs) emitted from diverse industrial processes and transport activities are recognized as major contributors to air pollution and harmful to human health, which is a subject of strict legislation [1]. VOCs can be completely degraded to carbon dioxide and water by applying the catalytic oxidation. As a typical catalyst, $CuO-CeO_2-ZrO_2$ oxides enjoy tremendous attentions since the superior redox properties and excellent thermal stability [2]. Co-precipitation, hydrothermal and sol-gel are usually adopted to prepare $CuO-CeO_2-ZrO_2$ oxides

1

which activities are strongly dependent on the structure [3, 4].

A proper pore structure in the catalyst can promote the migration and diffusion of the reactants and products, and it further facilitates the mass and thermal transfer [5]. A desired pore former, such as urea, KIT-6, oxalic acid and so on, which is capable of improving the catalyst structure and performance towards the VOCs removal, has captured broad research interest during the synthesis process of catalysts[6-8]. He et al. reported a mesoporous $CuCeO_x$ catalyst with high surface area synthesized using urea by a self-precipitation process, and the obtained $Cu_{0.3}Ce_{0.7}O_x$ catalyst achieved the 90% toluene and propanal conversion at 212 and 192 °C, respectively[6]. CeCu-HT3 catalyst with ordered mesopore structure prepared using a KIT-6 hard-template exhibited high catalytic activity and stability for toluene oxidation, owing to the abundant active oxygen species and superior reducibility[7]. Although some progresses have been made in the mesoporous catalysts by using chemical materials as pore formers for VOCs removal, the reports of hierarchically porous catalyst synthesized by a biological pore former are presently rather scarce.

Bacterial cellulose (BC) synthesized by some microorganisms is beneficial for the energy and environmental sustainability. Advantages of the BC including ultrafine three-dimension networks, chemical stability, high crystallinity and excellent compatibility have triggered awareness focused on the catalytic application, such as support and template [9-13]. Mesoporous TiO_2 networks synthesized by BC membrane enhanced photocatalytic activity compared to TiO_2 networks templated by eggshell membranes [9]. It was also reported that BC as a catalyst support could

provide a bonding site for the catalyst precursor and played an anchor role on the metal particles because of its surface hydroxyl groups [11]. Zhou et al. reported that BC nanofibers supported Pd was a highly efficient and recyclable catalyst for standard Heck coupling reaction [13]. However, studies on directly using BC as the pore former to synthesize the hierarchically porous complex metal oxide catalysts were scarcely reported, especially in the field of VOCs catalytic oxidation.

In this paper, two kinds of BC, namely coconut commodity (commercial BC) and cultured bacterial cellulose (cultured BC), are used as the bio-based pore formers to prepare hierarchically porous $CuCe_{0.75}Zr_{0.25}O_y$ catalyst by a modified sol-gel method. Based our previous studies [14-16], the relationships between the catalytic activities of VOCs (toluene and ethyl acetate) and the physico-chemical properties including the textural properties, active phase dispersion, reducibility and oxygen vacancy concentration are comprehensively explored.

2. Experimental

2.1. BC pretreatment

Two kinds of the BC, cultured BC and commercial BC, were selected as the pore formers in the sol-gel process. The cultured BC was screened from a traditional Chinese drink by our group, as described previously [17,18]. The cultured BC was dispersed preliminarily by a disintegrator and then homogenized using a high pressure homogenizer for 10 times at 100 MPa to obtain homogeneous dispersed suspension. The BC dispersion was centrifuged at a speed of 9000 rpm for 10 min, and the precipitate was used as the pore former.

3

The commercial BC was immersed in the deionized water for overnight and then filtrated. The filter cake was washed by deionized water for several times to remove sucrose. And then it followed the above cultured BC process for the commercial BC pretreatment.

2.2. Catalyst preparation

The molar ratio of Cu/(Ce+Zr) in Cu-Ce-Zr catalysts is fixed as 1:1, and Ce/Zr mole ratio is 3 according to our previous work [14]. $CuCe_{0.75}Zr_{0.25}O_y$ catalysts were prepared by a modified sol-gel method using the cultured BC or the commercial BC as the pore former. 10.09 g of $Cu(NO_3)_2 \cdot 3H_2O$, 13.56 g of $Ce(NO_3)_3 \cdot 6H_2O$ and 4.47 g of $Zr(NO_3)_4 \cdot 5H_2O$ were dissolved in 70 mL of ethanol at 80 °C to obtain Cu-Ce-Zr solution. 100 g of the cultured BC or the commercial BC was added into the solution, and stirred at 80 °C for 12 h to form gel. The gel was aged at room temperature for 48 h and dried at 80 °C for 12 h, and finally calcined at 550 °C for 2 h. The obtained catalysts prepared with cultured BC and commercial BC were denoted as Cul-BC and Com-BC, respectively.

The hierarchical pores in $CuCe_{0.75}Zr_{0.25}O_y$ catalyst were formed through a facilitated sol-gel process, as depicted in Fig. 1. Metal ions were firstly dissolved in ethanol at 50 °C, and then the BC was added into the ethanol solution at a stirring speed of 1800 rpm. The homogeneously dispersed suspension was obtained (Stage 1), which is considered to play an indispensable role in the formation of hierarchical pores in Cu-Ce-Zr ternary oxide mixture. The mixture was heated to 80 °C and kept for 3 h in order to achieve the ordered assembly. Along with the ethanol evaporation,

the metal ions were absorbed gradually on the surface of BC because of the interaction of the hydroxyl in ethanol and the hydrophilic radical in the BC. This ordered assembly process caused the development of persistent gel of corresponding metal cationic (Stage 2). The catalyst precursor with solid block structure was formed when the gel aged at room temperature for 48 h and dried at 80 °C for 12 h (Stage 3). The Cu-Ce-Zr catalyst with hierarchical pore structure could be finally obtained after removing the BC at 550 °C in air. The ultrafine three-dimension networks endow BC act as the pore former of mesopore and macropore. In addition, the sucrose molecules in BC were probably carbonized during the calcination at low temperature. The carbonized sucrose was probably responsible for the formation of micropore structure in $CuCe_{0.75}Zr_{0.25}O_y$ catalyst during the calcination at high temperature (Stage 4).

2.3. Catalyst characterization

N$_2$ adsorption-desorption isotherms were collected at -196 °C using an Autosorb-Iq-MP instrument (Quantachrome). Each sample was degassed at 300 °C for more than 4 h before measurement. The specific surface area of samples was calculated following the Brunauer-Emmett-Teller (BET) method, and average pore size was obtained by the BJH (Barett-Joyner-Halenda) method and NLDFT (non-local density functional theory) modeling.

X-ray diffraction (XRD) patterns were determined by DX-2700 X-ray diffractometer with Cu Ka radiation (λ=0.1541 nm, 40 kV, 30 mA) in the 2θ range of 5 °-85 ° (the step size of 0.06 °). The Scherrer's equation was used to calculate the average crystallite size. Raman spectra analysis was performed on HORIBA

5

LabRAM HR Evolution spectrometer with a confocal microprobe Raman system equipped an excitation laser line of 514 nm. The spectral range from 10 to 9000 cm-1 was collected with the step size of 100 nm at a resolution of 1 cm^{-1}.

H$_2$ temperature-programmed reduction (H$_2$-TPR) experiments were performed on PCA-140 instrument (Builder) equipped with TCD. Prior to the reduction, the catalyst (~200 mg) was pretreated in an Ar flow (50 mL/min) from room temperature to 500 °C with a rate of 20 °C/min for 1 h, then was treated in a reduction gas of 5 % /Ar with a flow rate of 50 mL/min from room temperature to 800 °C. The heating rate was controlled at 10 °C/min during the test.

The CuO dispersion measurement was also investigated on the same PCA-140 instrument. During the measurement process, the catalyst sample was subjected a complex treatment, that is combination process of reduction, oxidation and reduction. Firstly, the sample was pretreated from room temperature to 500 °C at a heating rate of 20 °C/min in flowing Ar (99.999 %, 30 mL/min) for 1 h. After the reactor was cooled down to room temperature, the reduction gas of 5 % H$_2$/Ar (30 /min) was introduced and then heated to 600 °C at a heating rate of 5 °C/min. Secondly, the reactor was cooled down to room temperature again in an Ar flow (30 mL/min) and kept for 30 min. The reduced sample was oxidized in a pure N$_2$O (99.999 %) flow with a flow rate of 30 mL/min to 60 °C for 1 h, and the sample was followed by treating in Ar (30 mL/min) for 1 h. Finally, the sample was again reduced under 5 % H$_2$/Ar (30 /min) from room temperature to 600 °C with a heating rate of 5 °C/min. The CuO dispersion (D) was calculated by D = 2 A$_2$/A$_1$, where A$_1$ is H$_2$ consumption

during the first reduction ($\mu mol \cdot g^{-1}$), A_2 is H_2 consumption during the second reduction ($\mu mol \cdot g^{-1}$), D is the CuO dispersion (%). The CuO average particle size was calculated by d_{CuO} (nm) = 1.1/D.

2.4. Catalytic activity measurement

Toluene and ethyl acetate were selected as the target pollutants for the removal effectiveness of the catalysts, and the reaction was performed in a fixed-bed reactor[16]. Approximately 0.8 g catalyst (20-40 mesh) was loaded into the reactor. The reaction temperature was monitored by a thermocouple located inside the catalyst bed. The reaction feed consisted of 1500 ppm of toluene or ethyl acetate in dry air with a total gas flow of 400 mL/min, space velocity (SV) of 24,000 h^{-1}. The reactor was heated from room temperature to 110 °C at a heating rate of 1 °C/min in flowing air and held at the temperature for 30 min before the catalyst testing. The compositions of inlet and outlet gas of the reactor were analysed by using a gas chromatograph (GC-2014, Shimadzu) with a flame ionization detector (FID, DB-35MS) for toluene and ethyl acetate analysis, and a TCD (AE. Porapak N) for CO_2 analysis. The conversion rates of target pollutants were calculated based on the concentrations of inlet and outlet gas. The selectivity towards CO_2 (or by-product ethanol) was calculated as the outlet concentration of CO_2 (ethanol)/total content of target pollutants converted to CO_2 (or ethanol).

3. Results and discussion

3.1. Catalyst structure properties

N_2 adsorption-desorption isotherms and the pore size distribution of CuI-BC and

7

Com-BC catalysts are shown in Fig. 2 (A) and Fig. 2 (B), respectively. The textural properties of the catalysts are summarized in Table 1. In Fig.2A, Com-BC and Cul-BC catalysts exhibit type Ⅱ isotherms with a H3 hysteresis loops, according to IUPAC classification. For Com-BC, the steep increase of adsorbed amount at low relative pressure ($P/P_0 < 0.1$) indicates the presence of a certain amount of micropores in this catalyst[19]. The hysteresis loops demonstrate the existence of mesopore and macropore in both Com-BC and Cul-BC[20-22]. Combined with the pore size distribution (Fig.2B), it is obvious that the Com-BC catalyst possesses hierarchically porous structure with micropore, mesopore and macropore simultaneously. Furthermore, the average pore size and S_{BET} of the Com-BC catalyst are much higher than those of the Cul-BC (Table 1).

The XRD patterns of the catalysts are exhibited in Fig. 3. Characteristic peaks of bulk phase CuO are detected at 2θ values of 35.7° and 38.8°, suggesting the aggregation of copper species. And the typical fluorite oxide characteristic peaks of CeO_2 are observed in all samples. Compared with CeO_2, the Cul-BC and Com-BC catalysts exhibit much broader and relative weaker diffraction peaks, and the peaks shift to higher 2θ values simultaneously. These results suggest that partial Cu^{2+} (0.72 Å) and/or Zr^{4+} (0.84 Å) incorporates into the lattice of CeO_2 (0.97 Å) to form lattice defects and oxygen vacancies, which can be further verified by the slight decrease of the CeO_2 lattice parameter and average crystallite size in the two catalysts (Table 2) [1,6,7,23].

The Raman spectra and oxygen vacancy concentration of Cul-BC and Com-BC

catalysts are shown in Fig. 4. It can be seen that pure CeO_2 have four distinct bands at 286, 455, 590 and 1180 cm^{-1}. The strong band at 455 cm^{-1} is attributed to the F_{2g} vibration mode of the fluorite structure of CeO_2[24]. The Raman peak centred at about 590 cm^{-1} is ascribed to the oxygen vacancies (O_v) in CeO_2, and the band at 1180 cm^{-1} is linked to the primary A_{1g} asymmetry of CeO_2[25,26]. While the weak band at 286 cm^{-1} that appears for CeO_2 is assigned to the rearrangement of oxygen atoms from their ideal fluorite lattice positions[27]. For the CuI-BC and Com-BC catalysts, the intensity of the peak at 455 cm^{-1} decreases significantly indicating the appearance of lattice distortion in CeO_2, which results from the incorporation of Cu^{2+} and/or Zr^{4+} into the CeO_2 lattice[28]. It is worth noting that the intensified band at 286 cm^{-1} for Com-BC suggests the promotion of the degree of oxygen atoms rearrangement. The intensity of the band at 590 cm^{-1} for Com-BC is obviously strengthened compared with the CeO_2, indicating the formation of the large amount of the oxygen vacancies. In addition, the relative concentration of the oxygen vacancies (O_v/F_{2g}) of the catalysts is calculated by the intensity ratio of the bands at 590 cm^{-1} and 455 cm^{-1} (Fig. 4). The O_v/F_{2g} value of Com-BC (1.6) is dramatically higher than that of the CuI-BC (0.1) which demonstrates abundant oxygen vacancies existing in the Com-BC catalyst.

H_2-TPR profiles of the catalysts are shown in Fig. 5, and the corresponding H_2 consumptions are listed in Table 3. It is obvious that the reduction peaks of the catalysts exhibit four peaks denoted as α (130-200 °C), $β_1$ (200-230 °C), $β_2$ (230-250 °C), and γ (250-300 °C), respectively. The α peak is ascribed to the

9

reduction of the highly dispersed copper oxide species strongly interacting with CeO_2[29,30]. The reduction of Cu^{2+} ions in the subsurface of CeO_2 lattice is responsible for the β_1 peak, and the β_2 peak is attributed to the reduction of Cu^{2+} ions in the bulk of CeO_2 lattice[24]. The γ peak is due to the reduction of bulk CuO, which is in accordance with the above XRD results. Compared with Cul-BC, Com-BC shows lower reduction temperature and higher H_2 consumption of α peak, indicative of better reducibility and more highly dispersed copper oxide species for Com-BC. Such a phenomenon demonstrates that the redox cycle between Cu^{2+}/Cu^+ and Ce^{3+}/Ce^{4+} is more facile to take place in Com-BC, which results from a stronger synergetic effect between CuO and CeO_2[1]. Higher content of well-dispersed copper oxide species existing in the Com-BC catalyst can also be evidenced by the CuO dispersion experiments. As shown in Table 2, the CuO dispersion (D) in Com-BC is 40.0%, whereas that in Cul-BC is 19.8 %. Moreover, the smaller CuO particles facilitate them easier to be reduced, which is consistent with the reduction temperature of α peak[4].

3.2. Catalyst performances

The toluene and ethyl acetate conversion (A), CO_2 selectivity (B) and by-product selectivity (C) over the Cul-BC and Com-BC catalysts are shown in Fig. 6. Com-BC exhibits higher activity for toluene abatement than Cul-BC. T_{10}, T_{50}, T_{90} and T_{100} (temperatures at 10 %, 50 %, 90 % and 100 % conversion rates are reached, respectively) of Com-BC are 156, 190, 209 and 220 °C , respectively, which are lower than those of Cul-BC. CO_2 selectivity (Fig. 6 B) synchronously increases with

the increase of toluene conversion. The similar trends are observed for the ethyl acetate conversion and CO_2 selectivity over the Com-BC and Cul-BC catalysts. No by-product is detected in the process of toluene oxidation, suggesting that the toluene can be completely degraded to CO_2 and H_2O. Ethanol is an only by-product during the process of ethyl acetate degradation at 120-180 °C (Fig. 6 C). At 160 °C, the maximum of the ethanol selectivity is obtained over the two catalysts. With the temperature further increasing, the ethanol disappears and the ethyl acetate is again completely degraded to expected products, CO_2 and H_2O.

The excellent activity of the Com-BC catalyst is mainly ascribed to the high concentration of oxygen vacancies, superior reducibility and hierarchically porous structure. The oxygen vacancies accelerate the adsorption and dissociation of oxygen molecules, which provide active centres for the formation of reactive oxygen species promoting the catalyst activity, and simultaneously improve the diffusion of lattice oxygen [7,27]. In addition, the highly dispersed CuO species strongly interacting with CeO_2 are mainly active sties for VOCs oxidation, and the synergetic effect between CuO and CeO_2 can weaken the Cu-O and Ce-O chemical bonds, which results in producing more reactive oxygen species and provides a facilitated redox process [7]. The hierarchical pore structure with micropore, mesoporore and macropore is also indispensable to the enhancement of the Com-BC activity. The developed pore structure in Com-BC catalyst boosts the contacting probability of VOCs molecules with active sites and hence promotes the migration and diffusion of the reactants and products. The resulting activities of Com-BC catalyst for the toluene and ethyl acetate

11

degradation are better than those of the other catalysts reported, with the comparisons showed in Table 4.

3.3. Catalyst stability

A series of experiments including the Com-BC and Cul-BC catalyst preparation and catalyst testing, have been repeated for four times. The toluene conversions and CO_2 selectivity of the repeated experiments are exhibited in Fig. 7. Almost the same results are obtained in the four repeated experiments, indicating that the resulting data are reliable.

The stabilities of Com-BC catalyst for the toluene and ethyl acetate oxidation were tested for 100 h, and the results are shown in Fig. 8. The temperatures of the complete degradation for the toluene and ethyl acetate were 220 °C and 170 °C, respectively. The conversion of toluene (220 °C) and ethyl acetate (170 °C) were continuously kept at 100 %, and no deactivation was observed in each of the tests. The results demonstrate that the hierarchically porous $CuO\text{-}CeO_2\text{-}ZrO_2$ catalyst prepared using commercial bacterial cellulose exhibits the superior stability.

4. Conclusion

Hierarchically porous $CuCe_{0.75}Zr_{0.25}O_y$ catalyst prepared using simple sol-gel process with environmentally-friendly commercial bacterial cellulose was achieved. The performances of Com-BC catalyst were better than those of Cul-BC catalyst and many catalysts reported. The complete degradation temperatures of the toluene and ethyl acetate for Com-BC catalyst were as low as 220 and 170 °C, respectively. No

deactivation was observed for Com-BC during the 100 h on stream in toluene (T_{100}=220 °C) and ethyl acetate (T_{100}=170 °C) oxidation. The excellent activity of Com-BC was ascribed to its more oxygen vacancies, stronger metal-oxides synergistic effect, and hierarchically porous structure.

Acknowledgments

References

[1] Y. Qin, X. Liu, T. Zhu, T. Zhu, Mater. Chem. Phys. 229 (2019) 32-38.

[2] Q.L. Zhang, L.S. Xu, P, Ning, J.J. Gu, Q.Q, Appl. Surf. Sci. 317(2014) 955-961.

[3] E. Moretti, M. Lenarda, P. Riello, L. Storaro, A. Talon, R. Frattini, A. Reyes-Carmona, A. Jimenez-Lopez, E, Appl. Catal. B-Environ. 129(2013) 556-565.

[4] D.W. Jeong, W.J. Jang, H.S. Na, J.O. Shim, A. Jha, H.S. Roh, J. Ind. Eng. Chem. 27(2015)35-39.

[5] R.S. Yuan, X.Z. Fu, X.C. Wang, P. Liu, L. Wu, Y.M. Xu, X.X. Wang, Z.Y. Wang, Chem. Mater. 18(2006)4700-4705.

[6] C. He, Y.K. Yu, L. Yue, N.L. Qiao, J.J. Li, Q. Shen, W.J. Yu, J.S. Chen, Z.P. Hao, Appl. Catal. B-Environ. 147(2014)156-166.

[7] G.L. Zhou, H. Lan, T.T. Gao, H.M. Xie, Chem. Eng. J. 246(2014)53-63.

[8] W.X. Tang, X.F. Wu, G. Liu, S.D. Li, D.Y. Li, W.H. Li, Y.F. Chen, J. Rare. Earth. 33(2015)62-69.

[9] D.Y. Zhang, L.M. Qi, Chem. Commun. 21(2005) 2735-2737.

[10] T.Zhang, Y.D. Zheng, S.M. Liu, L.N. Yue, Y. Gao, Y. Yao, J. Electroanal. Chem. 750(2015)43-48.

[11] S.S. Liu, W.N. Yan, X.C. Cao, Z.F. Zhou, R.Z Yang, Int. J. Hydrogen. Energ. 41(2016)5351-5360.

[12] J.Z. Yang, W.H. Tang, X.L. Liu, C. Chao, J.G. Liu, D.P. Sun, Int. J. Hydrogen. Energ. 38(2013)10813-10818.

[13] P.P. Zhou, H.H. Wang, J.Z. Yang, J. Tang, D.P. Sun, W.H. Tang, Ind. Eng. Chem. Res. 51(2012)5743-5748.

[14] S.M. Li, Q.L. Hao, R.Z. Zhao, D.L. Liu, H.Z. Duan, B.J. Dou, Chem. Eng. J. 285(2016)536-543.

[15] B.J. Dou, S.M. Li, D.L. Liu, R.Z. Zhao, J.G. Liu, Q.L. Hao, F. Bin, RSC Adv. 6(2016)53852-53859

[16] B.J. Dou, D.L. Liu, Q. Zhang, R.Z. Zhao, Q.L. Hao, F. Bin, J.G. Cao, Catal. Commun. 92(2017)15-18.

[17] C. Zhong., F. Li., M. Liu, X.N. Yang, H.X. Zhu, Y.Y. Jia, S.R. Jia, PLOS ONE. 9(2014) 1-9.

14

[18] C. Zhong, G.C. Zhang, M. Liu, X.T. Zheng, P.P. Han, S.R. Jia, Appl Microbiol Biotechnol. 97(2013) 6189-6199.

[19] C.S. Lee, J.Y. Lim, W.S. Chi, J.H. Kim, Facile, Nonhydrothermal, Electrochim. Acta. 173(2015)139-147.

[20] G.Z. Li, Z.H. Diao, J.D. Na, L. Wang, Chinese J. Chem. Eng. 23(2015)1655-1661.

[21] J.Z. Ma, C.Z. Zhu, J. Lu, H.B. Liu, L. Huang, T.H. Chen, D. Chen, Solid. State. Sci. 49(2015)1-9.

[22] Y. Shao, H.H. Chen, Y.B. Li, X.O. Ma, Chem. Eng. J. 276(2015)51-58.

[23] D.R. Sellick, A. Aranda, T. García, J.M. López, B.J. Solsona, A.M. Mastral, D.J. Morgan, A.F. Carley, S.H, Appl. Catal. B-Environ. 132-133(2013)98-106.

[24] T. Tsoncheva, G. Issa, T. Blasco, M. Dimitrov, M. Popova, S. Hernandez, D. Kovacheva, G. Atanasova, J.M. Lopez Nieto, Appl. Catal. A-Gen. 453(2013)1-12.

[25] Z.G. Liu, R.X. Zhou, X.M. Zheng, J. Natagas. Chem. 17(2008)125-129.

[26] A.P. Jia, G.S. Hu, L. Meng, Y.L. Xie, J.Q. Lu, M.F. Luo, J. Catal. 289(2012)199-209.

[27] X.L. Guo, J. Li, R.X. Zhou, Fuel. 163(2016)56-64.

[28] P. Yang, S.S. Yang, Z.N. Shi, Z.H. Meng, R.X. Zhou, Appl. Catal. B-Environ. 162(2015)227-235.

[29] C. He, Y.K. Yu, Q. Shen, J.S. Chen, N.L. Qiao, Appl. Surf. Sci. 297(2014)59-69.

15

[30] M. Zabilskiy, B. Erjavec, P. Djinovic´, A. Pintar, Chem. Eng. J. 254(2014)153-162.

[31] J. L. Li, Z. P. Qu, Y. Qin, H. Wang, Appl. Surf. Sci. 385(2016)234-240.

[32] J. M. Giraudon, A. Elhachimi, F. Wyrwalski, S. Siffert, A. Aboukais, J. F. Lamonier, G. Leclercq, Appl. Catal. B-Environ. 75(2007)157-166.

[33] L. S. Liu, Y. Song, Z. D. Fua, Q. Ye, S. Y. Cheng, T. F. Kang, H. X. Dai, Appl. Surf. Sci. 396(2017)599-608.
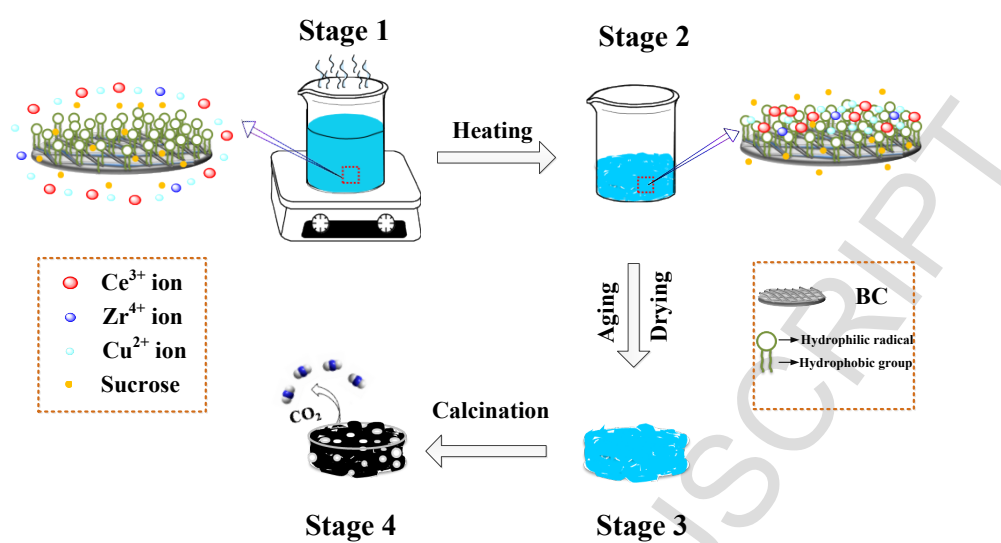
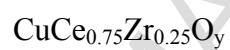[34] W. X. Tang, X. F. Wu, S. D. Li, W. H. Li, Y. F. Chen, Catal. Commun. 56(2014)134-138.

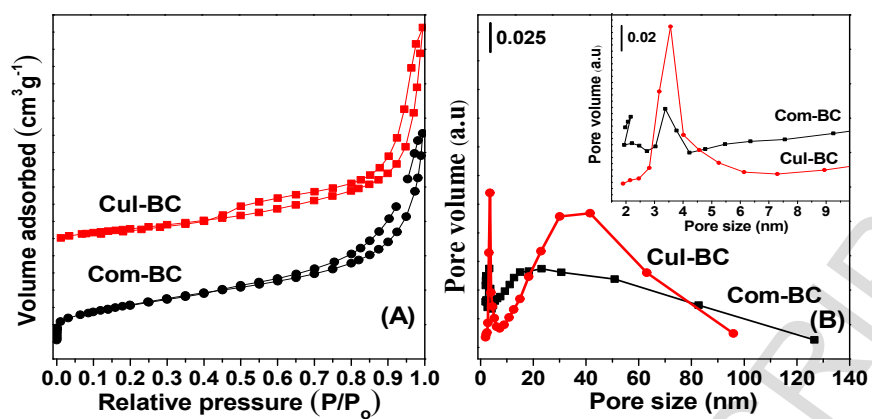**Fig. 1** Schematic illustration of the process for the formation of hierarchically porous

$CuCe_{0.75}Zr_{0.25}O_y$

Fig. 2 N$_2$ adsorption/desorption isotherms (A) and pore size distributions (B) of
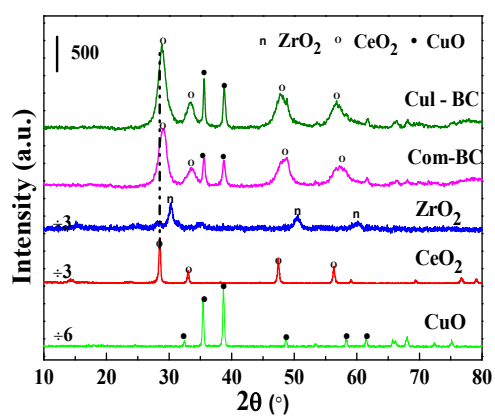
Cul-BC and Com-BC catalysts

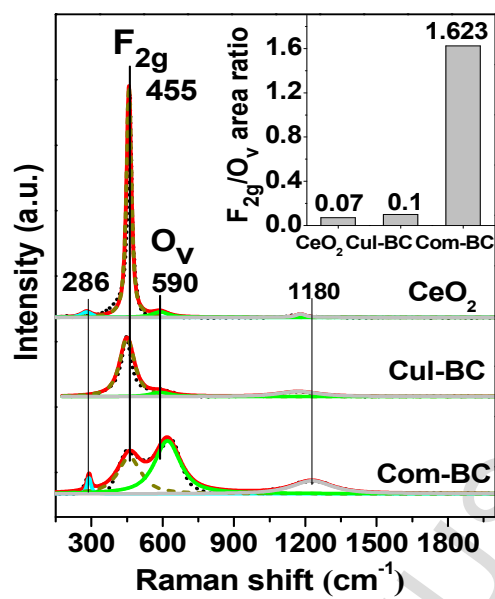**Fig. 3** XRD spectra of the Cul-BC and Com-BC catalysts
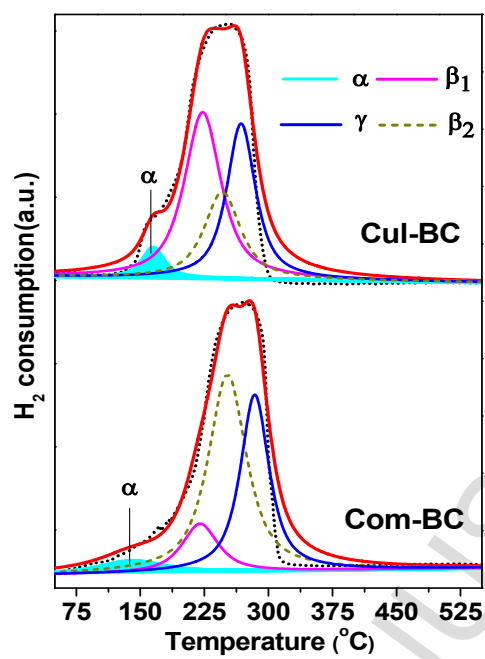
Fig. 4 Raman spectra of Cul-BC and Com-BC catalysts

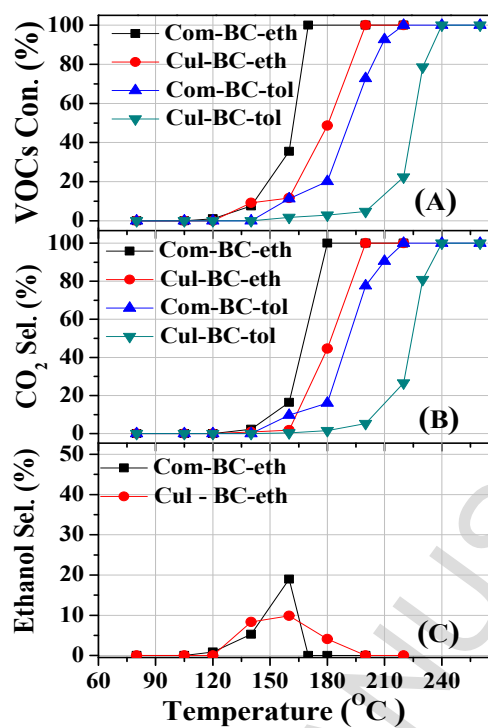**Fig. 5** H_2-TPR profiles of Cul-BC and Com-BC catalysts

Fig. 6 Toluene (-tol) and ethyl acetate (-eth) conversion (A), CO_2 selectivity (B) and

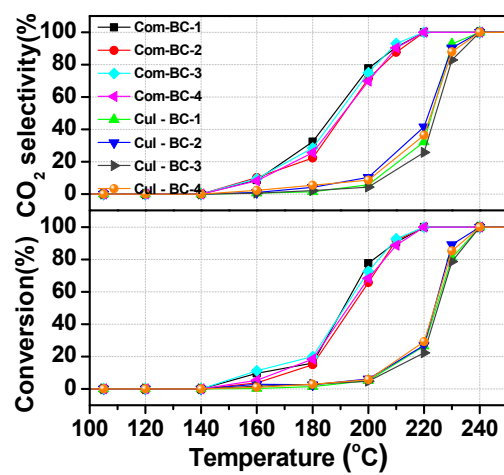the by-products selectivity (C) over Cul-BC and Com-BC catalysts

Fig. 7 Repeat experiments of toluene conversion and CO_2 selectivity over the catalysts

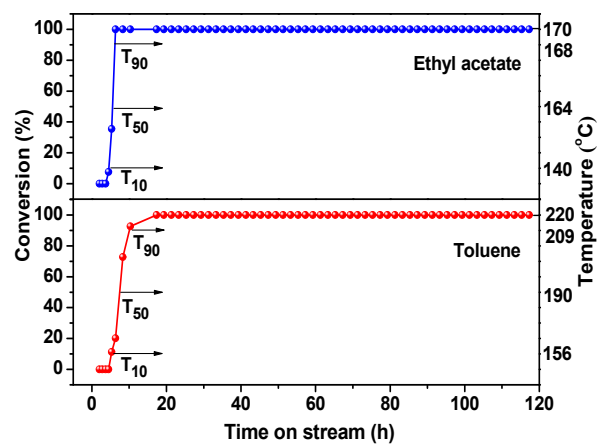**Fig. 8** Stability of the Com-BC catalyst for toluene and ethyl acetate as a function of time on the

stream

- Highly active CuO-CeO$_2$-ZrO$_2$ catalyst was prepared with bacterial cellulose.

- Com-BC prepared with commercial BC exhibits excellent activity and stability for VOCs oxidation.

- Hierarchically porous structure, abundant oxygen vacancies, and good reducibility lead to high activity of Com-BC.

Table 1 Textural properties of Cul-BC and Com-BC catalysts

Catalysts	Surface area $(m^2 \cdot g^{-1})$	Mean pore size (nm)	Pore volume $(cm^3 \cdot g^{-1})$
Cul-BC	28.1	11.3	0.10
Com-BC	39.9	88.3	0.09

Catalysts	Surface area $(m^2 \cdot g^{-1})$	Mean pore size (nm)	Pore volume $(cm^3 \cdot g^{-1})$
Cul-BC			

Table 2 CeO$_2$ lattice parameter, average crystallite size and CuO dispersion of catalysts

Catalysts	XRD		N$_2$O decomposition	
	Lattice parameter (Å)	Average crystallite size (nm)	D (%)	CuO average Crystallite size (nm)
Cul-BC	5.349	5.4	19.8	5.56
Com-BC	5.304	5.2	40.0	2.75
CeO$_2$	5.412	6.9	-	-

Table 3 H_2 consumption of the Cul-BC and Com-BC catalysts

Samples	H_2 consumption ($\mu mol \cdot g^{-1}$)				
	α peak	β_1 peak	β_2 peak	γ peak	Total
Cul-BC	105	984	721	505	2315
Com-BC	131	282	1312	721	2446

Table 4 Comparison of catalytic performances for toluene and ethyl acetate degradation

Catalysts	Pollutants	SV (h⁻¹)	Concentration (ppm)	T_{90} (°C)	Reference
Com-BC		24000	1500	209	This work
$Cu_{0.3}Ce_{0.7}O_X$		36000	1000	212	[6]
Ag/MnO_2	Toluene	20000	1000	212	[31]
$Mn_{0.5}Ce_{0.5}$-HL		60000*	1000	245	[8]
0.5 %Pd/LaFeO₃		15000	1800	221	[32]
Com-BC		24000	1500	168	This work
Lo-Co	Ethyl	240000	2000	200	[33]
Mn_5Co_5	acetate	120000	1000	194	[34]
$Mn_{0.5}Ce_{0.5}$-HL		60000*	1000	180	[8]

*: The unit of SV is mL·g·h⁻¹